International Journal of Applied Earth Observations and Geoinformation 114 (2022) 103084

Contents lists available at ScienceDirect

International Journal of Applied Earth Observations and Geoinformation

journal homepage: www.elsevier.com/locate/jag

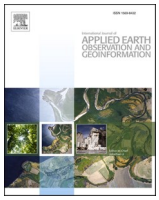

Earth observation for exposome mapping of Germany: analyzing environmental factors relevant to non-communicable diseases

Patrick Sogno [a,*], Claudia Kuenzer [a,b], Felix Bachofer [a], Claudia Traidl-Hoffmann [c,d]

[a] Earth Observation Center, EOC of the German Aerospace Center, DLR, Oberpfaffenhofen, 82234 Wessling, Germany
[b] Institute for Geography and Geology, University of Wuerzburg, Am Hubland, 97074 Wuerzburg, Germany
[c] Environmental Medicine, Faculty of Medicine, University of Augsburg, Stenglinstrasse 2, 86156 Augsburg, Germany
[d] Institute of Environmental Medicine, Helmholtz Center Munich, German Research Center for Environmental Health, Augsburg, Germany

ARTICLE INFO

Keywords:
Earth observation
Remote sensing
Public health
Green space
Noise pollution
Light pollution
Air pollution
Exposure
Non-communicable diseases
Myocardial infarction

ABSTRACT

Non-communicable diseases – NCDs – (e.g., asthma, cancer, or diabetes) are a major concern for society and medicine. According to the World Health Organization, NCDs are responsible for > 70 % of global premature deaths. Apart from increasing mortality, these diseases strain one's immune system which leads to higher susceptibility to transmittable diseases. NCD-susceptibility depends on the genome (genetic predisposition), behavior (lifestyle), and exposome of a person. The exposome is a composition of environmental parameters such as exposure to air pollution, noise, extreme temperatures, or surrounding greenness. Using Earth Observation data, the majority of factors making up the exposome can be monitored over long periods of time at high resolution and with nearly global coverage. Still, exposome maps and products communicating NCD risk are not widely available. In this study, we utilize eight land surface datasets (distance to green spaces, distance to blue spaces, temperature, noise from industry, as well as road, rail, and air traffic, and light pollution) as well as two air pollution datasets ($PM_{2.5}$ and NO_2) to map health-relevant environmental exposure. We use an established cumulative approach and incorporate exposure-response relationships from scientific literature to map environments that impact public health for the complete area of Germany. We present results communicating exposure relevant to myocardial infarction risk. The methodology is transferable to other NCDs and other areas of interest. In the context of the global health burden from NCDs and ongoing global change, this approach supplies findings for communicating health-relevant exposure.

1. Introduction

1.1. Attribution of environmental factors with non-communicable diseases

Diseases that cannot be transferred between hosts are considered non-communicable. The likelihood of non-communicable disease (NCD) onset is dependent on the genome, behavior, and environmental factors commonly aggregated to the term exposome. Apart from their effect on the well-being of individuals, NCDs have an impact on public health. They affect an entire society by reducing economic productivity and increasing pressure on healthcare institutions (Sogno et al., 2020).

As reported by the World Health Organization (WHO), 40 million of the 56 million global deaths in 2015 were due to NCDs. It is further estimated that up to 80 % of those deaths could have been prevented by decreasing exposure and vulnerability to NCD-risk factors (World Health Organization, 2021).

Over the last years, a growing number of works related NCD onset and severity to environmental factors (Breiteneder et al., 2019; Ring et al., 2014; Turner et al., 2017). In Sogno et al., 2020, we provide an overview of studies concentrating on this issue. Studies that include Earth Observation (EO) data alongside medical data are reviewed for the timeframe 2000–2020. From this review, it could be seen that especially air pollution parameters like particulate matter with a diameter of up to 2.5 μm ($PM_{2.5}$), and nitrogen dioxide (NO_2), are often investigated and associated with a range of NCDs. These factors are produced mainly in the combustion processes of vehicles and power plants, as well as in the production processes of factories and agriculture. Additionally, multiple land surface parameters (foremost greenness, traffic noise, light

* Corresponding author.
E-mail addresses: patrick.sogno@dlr.de (P. Sogno), claudia.kuenzer@dlr.de (C. Kuenzer), felix.bachofer@dlr.de (F. Bachofer), claudia.traidl-hoffmann@tum.de (C. Traidl-Hoffmann).

https://doi.org/10.1016/j.jag.2022.103084
Received 29 July 2022; Received in revised form 21 October 2022; Accepted 27 October 2022
Available online 31 October 2022

pollution, and temperature) have been attributed to NCD occurrence and mortality (Fig. 1). In the case of greenness, which is often seen as synonymous with vegetation exposure, most works attest a positive effect on human health. Only in articles that concentrate on allergic reactions, vegetation was found to increase NCD risk (Sogno et al., 2020).

1.2. Earth observation for non-communicable disease research

Studies that include both geographical and medical data are predominantly based on medical cohorts. Most cohort-based studies are methodologically quite similar: For geographically explicit points environmental data is gathered. The correlation of an environmental factor to an NCD or other medically relevant parameters is evaluated. This approach can identify attributions of environmental factors and NCDs, but it cannot portray the spatial distribution of such factors (Sogno et al., 2020).

EO, particularly satellite remote sensing, offers vast archives of freely accessible satellite data for high-frequency monitoring of health-relevant environmental parameters (Aschbacher, 2017; Zhu et al., 2019). This data riches can be used to map environmental exposure and identify adverse environments. However, so far only a few studies have attempted this. These works mostly concentrate on the assessment of environmental exposure and the quantification of health risk due to environmental exposure. The health outcome in focus varies among studies. Some focus on mortality (e.g., Gariazzo et al., 2021; Mueller et al., 2017; Sicard et al., 2011), while others concentrate on hospital admissions (e.g., Scherber et al., 2014). The exposure to adverse environmental parameters is mapped on the level of small administrative areas (e.g, Mueller et al., 2017; Sabrin et al., 2020; Scherber et al., 2014; Tomlinson et al., 2011) or in a gridded format ranging from several meters (e.g., Gariazzo et al., 2021) to multiple kilometers (e.g., Sicard et al., 2011) pixel size. Some studies solely map exposure (Sicard et al., 2011), while others include data on lifestyle differences (e.g., Mueller et al., 2017) or include socio-economic data that may impact health risk (e.g., Gariazzo et al., 2021; Scherber et al., 2014). This increases thematic depth but may reduce transferability for socio-economic variables that are mostly provided by local census bureaus and may differ from country to country and even from city to city.

Complementing the existing body of research, this study aims to map adverse environments using environmental factors associated with NCD onset and mortality based on epidemiological evidence (Table 1). This allows for spatial characterization of the NCD-specific exposome. Within this study, we concentrate on Myocardial Infarctions (MI), but the proposed approach is transferable to other NCDs based on the relative risk (RR) values in Table 1. In the following, we present the used data and methodology for exposome mapping. We advance on previous works by accounting for long-term exposure to a large array of environmental factors. We include several land surface parameters (green and blue space availability, land surface temperature (LST), nighttime light (NTL), and noise pollution), as well as harmful air pollution factors (NO_2, $PM_{2.5}$).

2. Study area

We perform our calculations for all of Germany. As showing the intricacies of urban morphology and small-scale spatial patterns of our input datasets would exceed the frame of this paper, we show them exemplary for a focus region. For this, we chose Augsburg, a medium-sized city in Bavaria, southern Germany (Fig. 2). The focus area consists of the city itself, as well as the adjacent counties (Landkreis Augsburg and Landkreis Aichach-Friedberg) and is located at 48.08° to 48.65° N, and 10.49° to 11.31° E. The entire focus area comprises a population of ~ 680,000, nearly half of this population (~ 300,000) resides within the city of Augsburg. Even though the surrounding areas are more sparsely populated than the city itself, they are well connected via roads and public transport and offer all local amenities (Neumeier, 2013). Fig. 2 portrays the land cover and urban morphology of the area.

Regarding the rest of the study area, Germany is a developed country

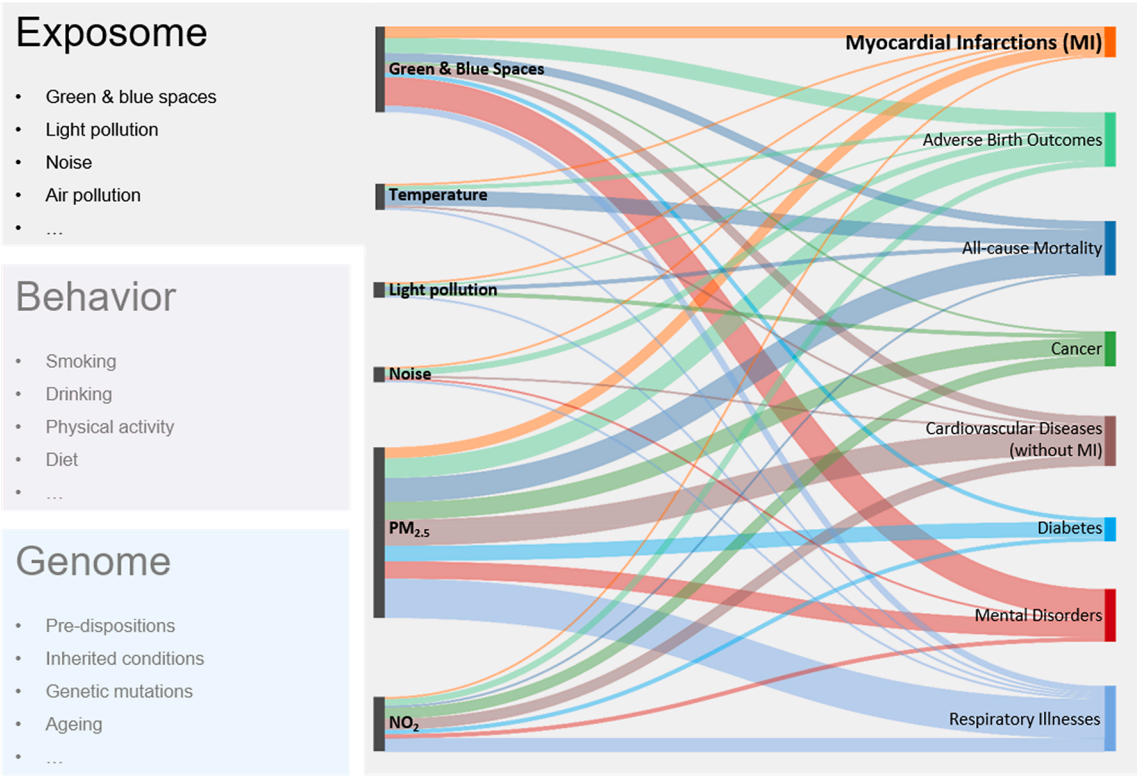

Fig. 1. Relevant spheres for NCD research. Of the three spheres involved, EO can give information on the exposome. Associations between environmental factors and specific NCD groups have been found in previous studies. This figure is based on a literature review on EO for NCD research and was adapted from Sogno et al., 2020.

Table 1
Disease-specific risk values for environmental factors. Factors are given as relative risk (RR) if not specified differently. Not all factors have reported RR values. Here, we provide odds ratios (OR), or hazard ratios (HR). If not specified differently, values are given for 10 μg/m^3 increment increases.

NCD	Lack of Green or Blue Spaces	Temperature	Light Pollution	Noise	$PM_{2.5}$	NO_2
Myocardial Infarctions (MI)	**1.121** per −1 unit increment of NDVI (Lee et al., 2020)	**1.016** per 1 °C increase (Sun et al., 2018)	**1.06** if short sleep (Grandner et al., 2010)	**1.04** per 10 dB increment (Liu et al., 2022)	**1.025** (Mustafić et al., 2012)	**1.011** (Mustafić et al., 2012)
Adverse Birth Outcomes	−16.3 g birth weight for interquartile range decrease in surrounding greenness (Villeneuve et al., 2022)	OR: 1.028 for an interquartile increase in temperature (Son et al., 2019)	OR: 1.07 and 1.12 for medium and high light pollution, respectively (Windsperger et al., 2022)	−19 g birth weight per 6 dB increment (Gehring et al., 2014)	1.03–1.22 for interquartile range increase during the second trimester (Ha et al., 2014)	−13.78 g birth weight (Huang et al., 2015)
All-cause Mortality	HR: 0.96 per 0.1 increment NDVI in 500 m buffer (Rojas-Rueda et al., 2019)	1.08–1.15 during heat waves (Schifano et al., 2009, p. 20)	1.10 if short sleep (Grandner et al., 2010)	1.01 per 10 dB increment (Cai et al., 2021)	1.08 (Chen and Hoek, 2020)	1.02–1.06 (Huangfu and Atkinson, 2020)
Cancer	1.148 per −1 unit increment of NDVI (Lee et al., 2020)	Mortality: 1.69 (low temperature), 2.57 (high temperature variation) (Kim et al., 2018)	1.726 at 25 % vs 75 % exposure quartile (Kim et al., 2017)	HR: 1.18 per 10 dB increment (Roswall et al., 2017, p. 20)	1.33 (Pun et al., 2017)	OR: 1.06 (Chen et al., 2015)
Cardiovascular Diseases (without MI)	1.049–1.072 if NDVI < 3rd quartile (da Silveira and Junger, 2018)	0.92–1.06 per 1 °C increment increase (Lin et al., 2011)	1.06 if short sleep (Grandner et al., 2010)	1.08 per 10 dB increment (Van Kempen et al., 2018)	1.08 (Chen and Hoek, 2020)	0.983–1.031 per 10 ppb increment (Shin et al., 2022)
Diabetes	OR: 1.389 (Twohig-Bennett and Jones, 2018)	Short-term: 1.07 per 1 °C increment increase (Song et al., 2021)	HR: 1.33 if short sleep (Holliday et al., 2013)	1.08–1.11 per 10 dB increment (Dendup et al., 2018)	1.25 (He et al., 2017)	OR: 1.12–1.19 (Shin et al., 2019)
Mental Disorders	1.042–1.333 for the lowest NDVI compared to the highest (Engemann et al., 2019)	1.079 for extreme heat (Sun et al., 2021)	OR: 1.07–1.19 (Paksarian et al., 2020)	2.0–4.0 (WHO Regional Office for Europe, 2009)	1.18 (Liu et al., 2021)	1.037 (Borroni et al., 2022)
Respiratory Illnesses	1.387 per −1 unit increment of NDVI (Lee et al., 2020)	1.183 during heatwaves (Cheng et al., 2019)	1.52 if short sleep (Bakour et al., 2020, p. 202)	1.038 per 1 dB increment (Tobías et al., 2001)	1.16 (Chen and Hoek, 2020)	1.03 (Huangfu and Atkinson, 2020)

with a population of ∼ 80 million people. It has a mostly oceanic to warm summer humid continental climate (Koeppen-Geiger: Cfb / Dfb) (Beck et al., 2018; Kottek et al., 2006). Although summers are generally mild, extreme heat events have been recorded more frequently over the last years. During these events, air temperature (AT) can rise over 30 °C at day and stay above 20 °C at night. The climate is humid throughout the year. There is considerable industrial activity, especially in the Ruhr valley in the west and along the Rhine. Although large parts of Germany are urbanized, there is substantial forest cover, foremost in the uplands in the country's center and south and along the southern border.

3. Available data

We utilize EO data portraying the health-relevant environmental factors presented in Section 1 to map adverse environments. We concentrate on MI and utilize the RR per increment values shown in Table 1, which is based on epidemiological evidence. We consider 5-year mean values for 2015–2019 to best represent the long-term Exposome in a "normal" situation (i.e. non-COVID). All used datasets used to map adverse environmental conditions are listed in Table 2 and pre-processed layers are shown in Fig. 3. Parameters that are not available for the entire study period are included from the first available date forward. Of the datasets used, green and blue space availability and noise pollution are not globally available. However, substitutes with similar properties are either available or producible using existing workflows. We reproject and resample all layers to 100 m spatial resolution in EPSG:3035. For upsampled layers, the mean pixel value of the original smaller pixels is used for the new coarser resolution raster. For downsampled layers, we utilize bilinear interpolation. Both resampling methods are common practice (Guzinski and Nieto, 2019; Manjarrés, 2009; Teoh et al., 2008).

3.1. Land surface parameters

Green and blue spaces are rasterized based on the Copernicus Corine Land Cover Classification from 2018 (European Environmental Agency, 2022a). From the resulting binary layer, green and blue space impact is approximated using a Kernel Density Estimation (KDE). By using a KDE, we gain a dataset with values ranging from 0 (no green or blue space) to 1 (green or blue space). We set the maximum radius of this KDE to be 1 km. This radius roughly reflects the positive impact green and blue spaces have on their neighborhood. As green and blue spaces are a documented positive influence on human health and the absence of such areas is associated with NCDs, we reclassify the layer to show an absence of blue or green spaces (0 = available; 1 = not available).

Heat stress is approximated using MODIS LST. A long-term mean is calculated based on all summer observations (July-September) for 2015–2019 and converted to °C. AT measurements would be preferable to approximate heat stress. However, due to the low availability of AT measurement stations in the study area, we use LST. The difference between AT and LST has been studied in comparable settings (Schwarz et al., 2012).

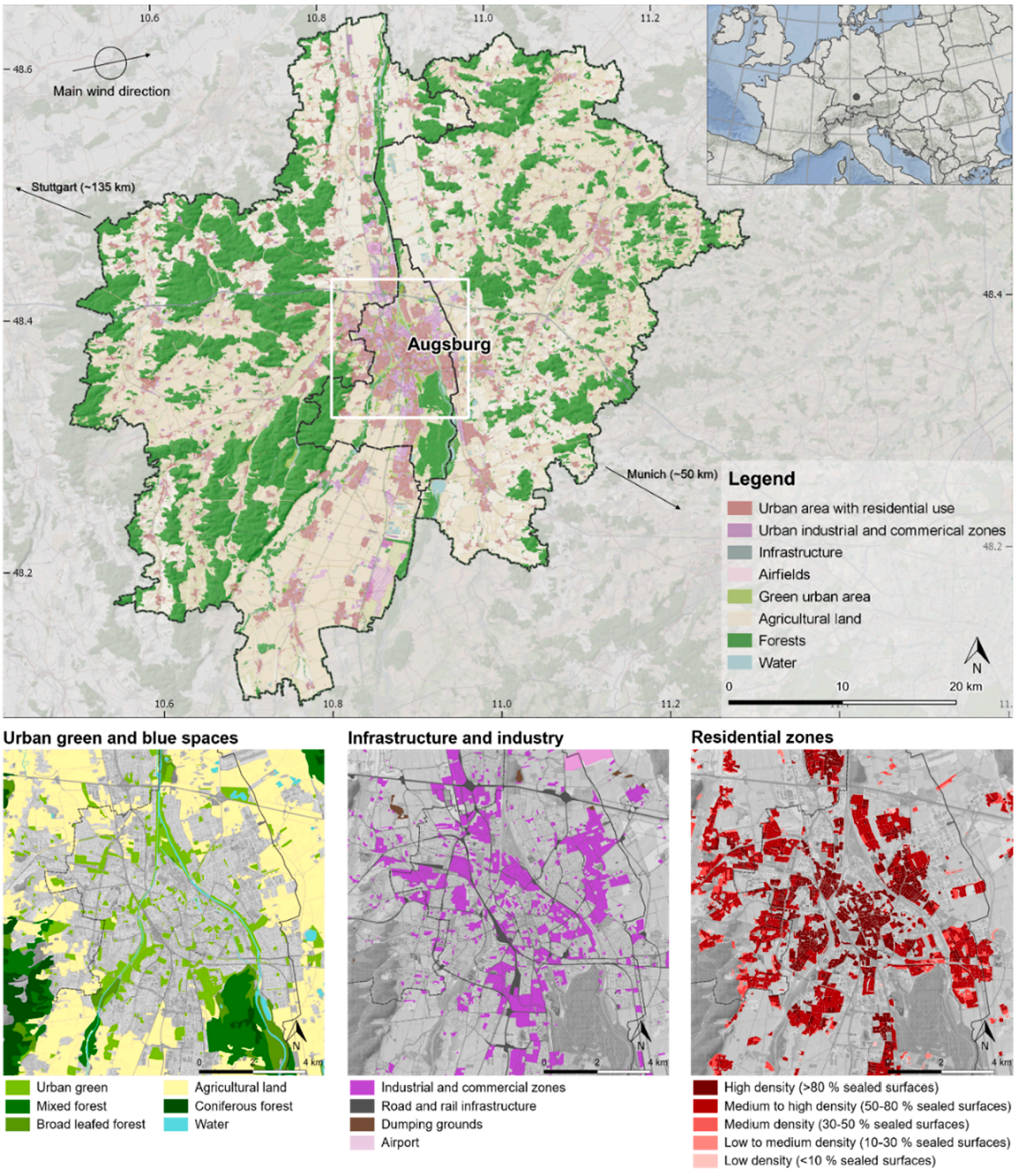

Fig. 2. Overview of Augsburg and adjacent counties. Copyright used data: European Environmental Agency, OpenStreetMap contributors. Wind direction: (Jacobeit, 1990).

Results indicate that LST is generally 2–3 K lower than AT. Going forward, we have to be aware of this possible underestimation and its impact on the cumulative exposure calculation.

NTL is included based on a Suomi NPP VIIRS Day-Night Band (DNB) composite. We calculate the long-term mean for 2015–2019.

Traffic and industry noise pollution is derived from datasets provided by the German Environment Agency (Umweltbundesamt, 2022a). The datasets for noise pollution from road, rail, and air traffic, as well as industrial are modeled at 10 m resolution based on field measurements carried out in 2017. It should be noted that traffic noise estimates are not produced for every street, only for main roads. We aggregate the cause-specific datasets to one maximum noise level layer.

Table 2
Considered Earth Observation parameters.

Parameters	Spatial resolution	Temporal resolution	Time frame	Source
Land surface				
Green and blue spaces	100 m	static	static (2018)	CORINE Land Cover [1]
Temperature	1,000 m	daily	2015–2019	MODIS (Collection 6) [2]
Light pollution	500 m	16 days	2015–2019	VIIRS [2]
Noise	10 m	static	static (2017)	(Umweltbundesamt, 2022a)
Atmosphere				
$PM_{2.5}$	1,000 m	monthly	2015–2019	(van Donkelaar et al., 2021)
NO_2	1,000 m	yearly	2015–2019	(Cooper et al., 2022)

[1] (European Environmental Agency, 2022a).
[2] Datasets accessed via Google Earth Engine (Gorelick et al., 2017).

3.2. Atmospheric parameters

We incorporate modeled surface $PM_{2.5}$ data by (van Donkelaar et al., 2021) as well as NO_2 data by (Cooper et al., 2022). Both datasets are available freely and globally at ~ 1 km resolution. The modeled $PM_{2.5}$ values are based on MODIS atmospheric optical depth (AOD) data along with ground-based AOD and $PM_{2.5}$ measurements and the GEOS-Chem atmospheric chemistry model (van Donkelaar et al., 2021). NO_2 surface data is based on the OMI and TROPOMI observations (Cooper et al., 2022).

4. Methodology

4.1. Data preparation

Following common practice (e.g., (Mueller et al., 2017; Sicard et al., 2012)), all pre-processed exposure datasets are converted to NCD-specific RR values (Fig. 4). RR = 1 means that exposure to a certain environmental factor does not affect the medical outcome, while values > 1 mean that there is an excess risk due to exposure. Values and increments used in our methodology are based on epidemiological evidence (Table 1). For clarification, consider the RR value for MI attributed to $PM_{2.5}$ exposure in Table 1: Per exposure increase of 10 μg/m^3, RR rises by a factor of 1.025. This means that MI risk is 2.5 % higher per 10 μg/m^3 increment.

Accordingly, we calculate RR increment as:

$$RR_i = R_i^{\rho_i} \quad (1)$$

Here, RR_i is the RR value for an exposure factor i. It is calculated as the RR value per increment from Table 1 (R_i) by the power of the concentration increment (or whatever other increment applies to exposure factor i) (ρ_i). We apply Equation (1) for the following exposures: LST, noise, $PM_{2.5}$, and NO_2. For lack of green and blue spaces, we reclassify values to a normalized raster with a minimum value of 1 and a maximum value of 1.121, as per values given in Table 1. Lastly, the RR due to NTL is approximated via the impact it has on sleep duration. As reported by (Patel, 2019), an increase of 10 nW/(cm^{2}sr) leads to a 2.19 % increase in reported insufficient sleep (<7h). RR from insufficient sleep is given in Table 1. Calculation from NTL to RR can be expressed as:

$$RR_i = (1 - \rho_i \cdot 0.029) + (\rho_i \cdot 0.029 \cdot R_i) \quad (2)$$

In Equation (2), RR_i, R_i, and ρ_i are defined the same as before. R_i is given in Table 1. The calculation takes into account that not all are affected by NTL-induced sleep deprivation and approximates a RR of 1 for all unaffected. In this way, we can express RR due to NTL-induced insufficient sleep for MI.

4.2. Cumulative exposure impact calculation

We adopt the methodology of (Sicard et al., 2012) for exposure impact calculation. Due to the different exposure-response relations of each environmental factor and human health, they formulate a cumulative approach given in Equation (3) in an adapted format:

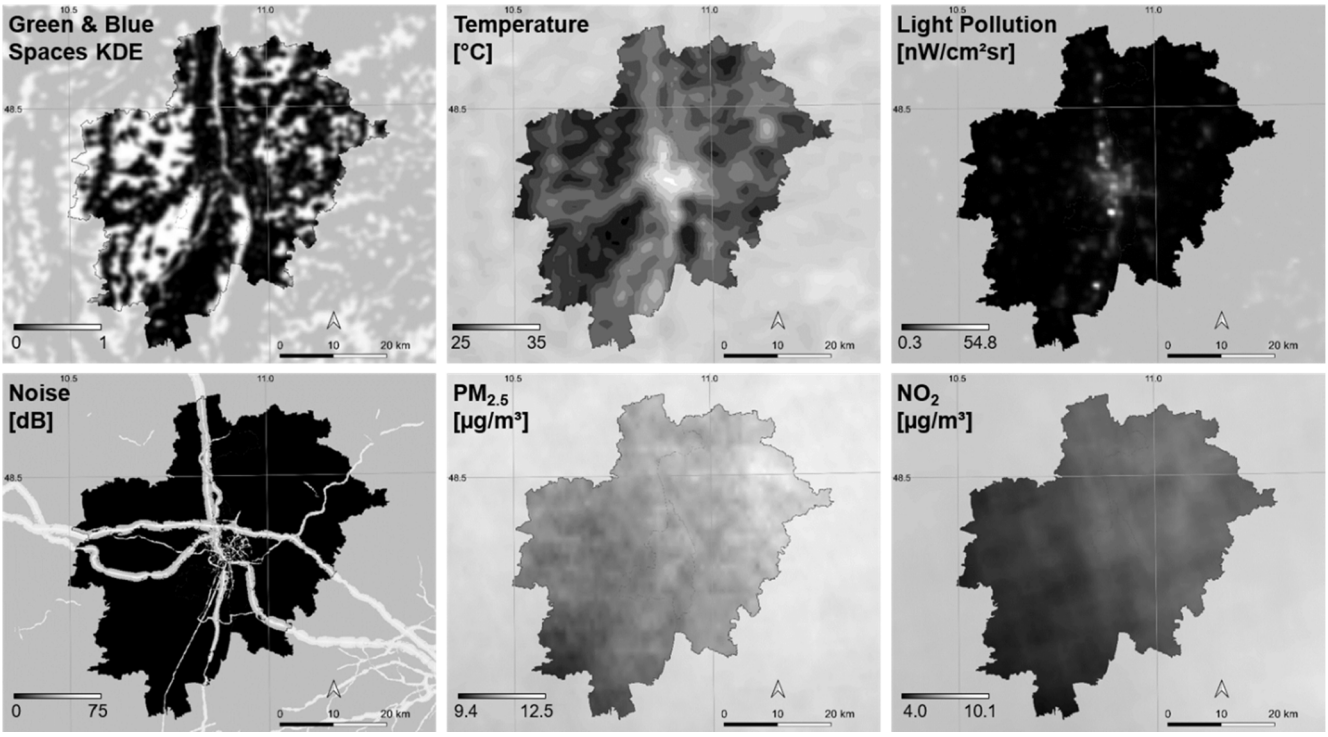

Fig. 3. Pre-processed exposure layers for the focus area of Augsburg.

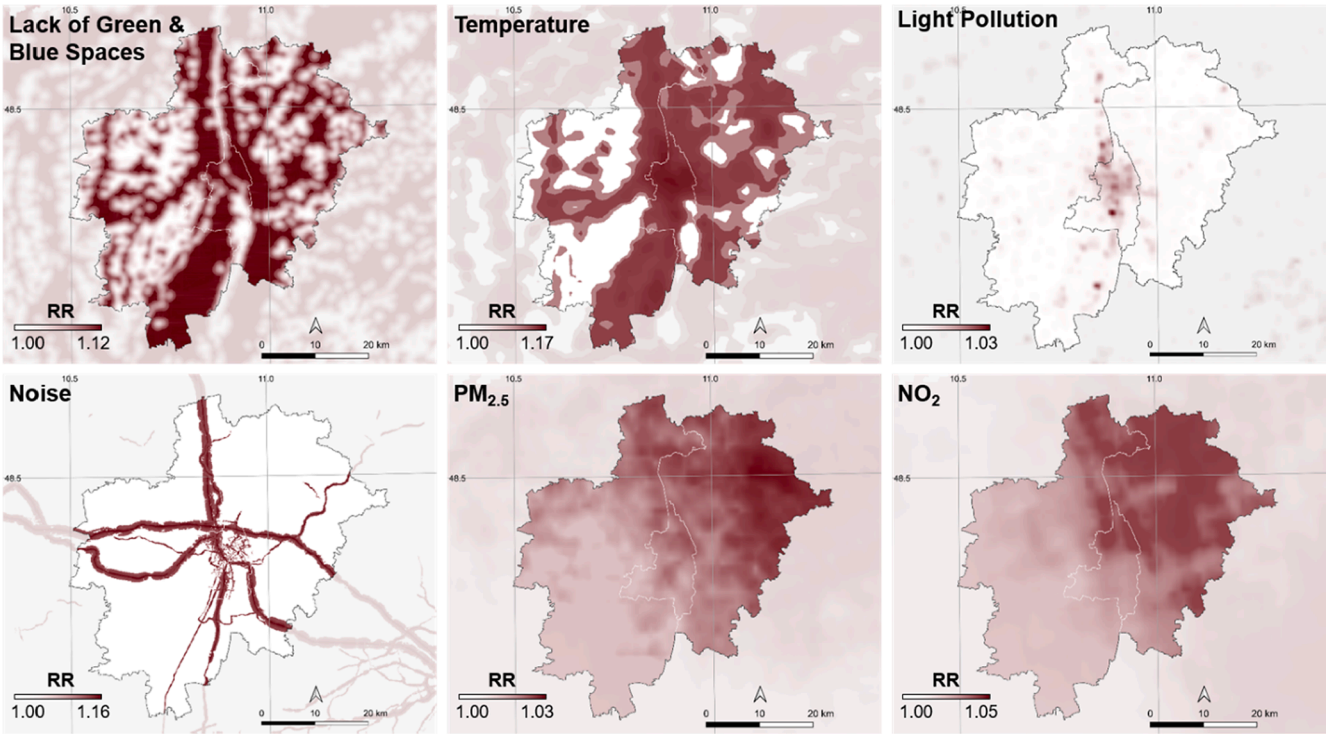

Fig. 4. Overview of exposure layers in RR format for MI in the focus area. Scaling varies and is given in quantiles so that spatial patterns are easily visible.

$$\text{Cumulative Exposure Impact} = \sum_{i=1}^{n} (RR_i - 1) \quad (3)$$

Here, RR_i is an exposure factor rescaled to relative risk concerning myocardial infarction as presented in Table 1. The value i goes from 1 to the number of included exposure factors (n = 9). Following the reasoning of (Sicard et al., 2012), values > 0 stand for increased health burden compared to a hypothetical "normal" situation, where RR = 1 for all exposure factors. While (Sicard et al., 2012) exclusively focus on short-term air pollution impact, our approach uses 5-year means. We thereby consider the findings of (Beverland et al., 2012), who indicate that long-term exposure has much higher associations with health response than short-term exposure. We further expand on the approach of (Sicard et al., 2012) by also accounting for land surface parameters. A full workflow, showing preprocessing and exposure calculation is provided in Fig. 5.

5. Results

At this point, the exposure maps we provide are merely a tool for communicating the environmental impact on human health burden. The actual NCD risk depends on a combination of factors, as briefly explained in Section 1. We base our exposure impact levels on those proposed by (Sicard et al., 2012). Specifically, we classify values of ≤ 0.09 as "very low", > 0.09 – ≤ 0.22 as "low", > 0.22 – ≤ 0.36 as

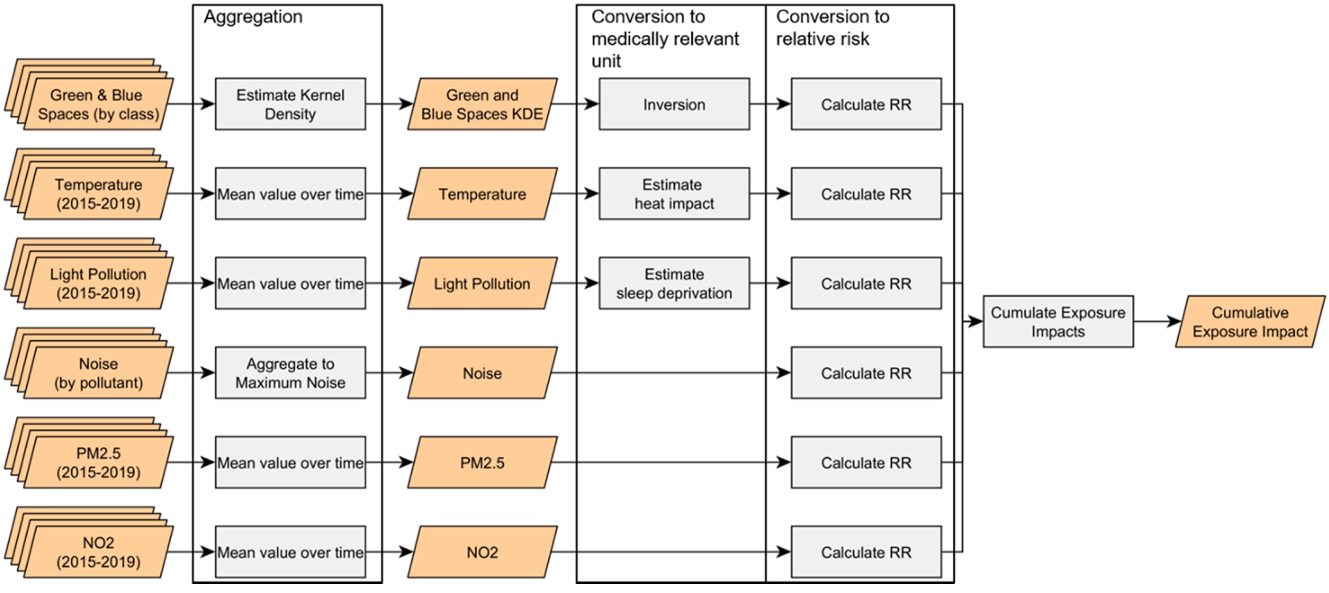

Fig. 5. Workflow for cumulative exposure impact calculation. The usage of multiple input datasets is shown as stacks.

"moderate", > 0.36 – ≤ 0.43 as "high", and > 0.43 as "very high" cumulative exposure impact. In the respective graphics (Fig. 6, Fig. 7), the choice of a continuous color gradient makes nuances in exposure impact visible. As (Sicard et al., 2012) already stated, these levels are essentially arbitrary and foremost serve for communicating the potential health burden from the cumulative exposure impact.

5.1. Focus area

Using Augsburg as an example, we demonstrate the ability of our approach to map small-scale differences in exposure. For data on land use and population numbers, we rely on the Urban Atlas of 2018 by (European Environmental Agency, 2022b). From the spatial patterns visible in Fig. 6, we see elevated exposure impact values in the urban center, while in the rural surroundings of Augsburg cumulative exposure is mostly "very low" to "low".

The impact of several included exposure parameters (Fig. 4) is visible in the cumulative exposure. We can for example identify the impact of noise pollution along the main transport axes from west to east and north to south. East of the city, exposure values are higher than west of the city, following the RR spatial patterns of $PM_{2.5}$, NO_2, and heat (Fig. 4). Areas of "very low" exposure impact are confined to forests, lakes, and rivers around the city, where noise pollution, temperature, and air pollution values are low. There is a visible gradient from low-exposure areas around the city to higher values within it, where high exposure values coincide with areas with high noise pollution, a lack of green and blue spaces, and high temperatures.

Taking into account the land use maps of Fig. 2, we see that within the city, "high" and "very high" cumulative exposure is concentrated around busy streets, railways, and areas of industrial land use. Areas of "very low" and "low" exposure on the other hand are mostly found along the city limit, as well as in recreational areas (e.g., city parks). For built-up areas of the focus region, we see "high" and "very high" values predominantly in the city's northwest, reaching into the center along the main transport axes. Here, land use is mostly industrial or commercial. In the center of the zoomed-in views in Fig. 6, which coincides with Augsburg's city center, exposure is mostly "moderate". Individual strips and dots of higher exposure impact exist along busy streets and at junctions, but the majority of residential housing is not impacted by these exposures. Within the central urban area, most people live in areas of "moderate" exposure (~ 69 %). 13 % of the population even lives in areas of "low" exposure impact. Still, the share of people who live in "high" or "very high" exposure impact areas (~ 18 %) is considerable as this share translates to > 45,000 people with severely increased health

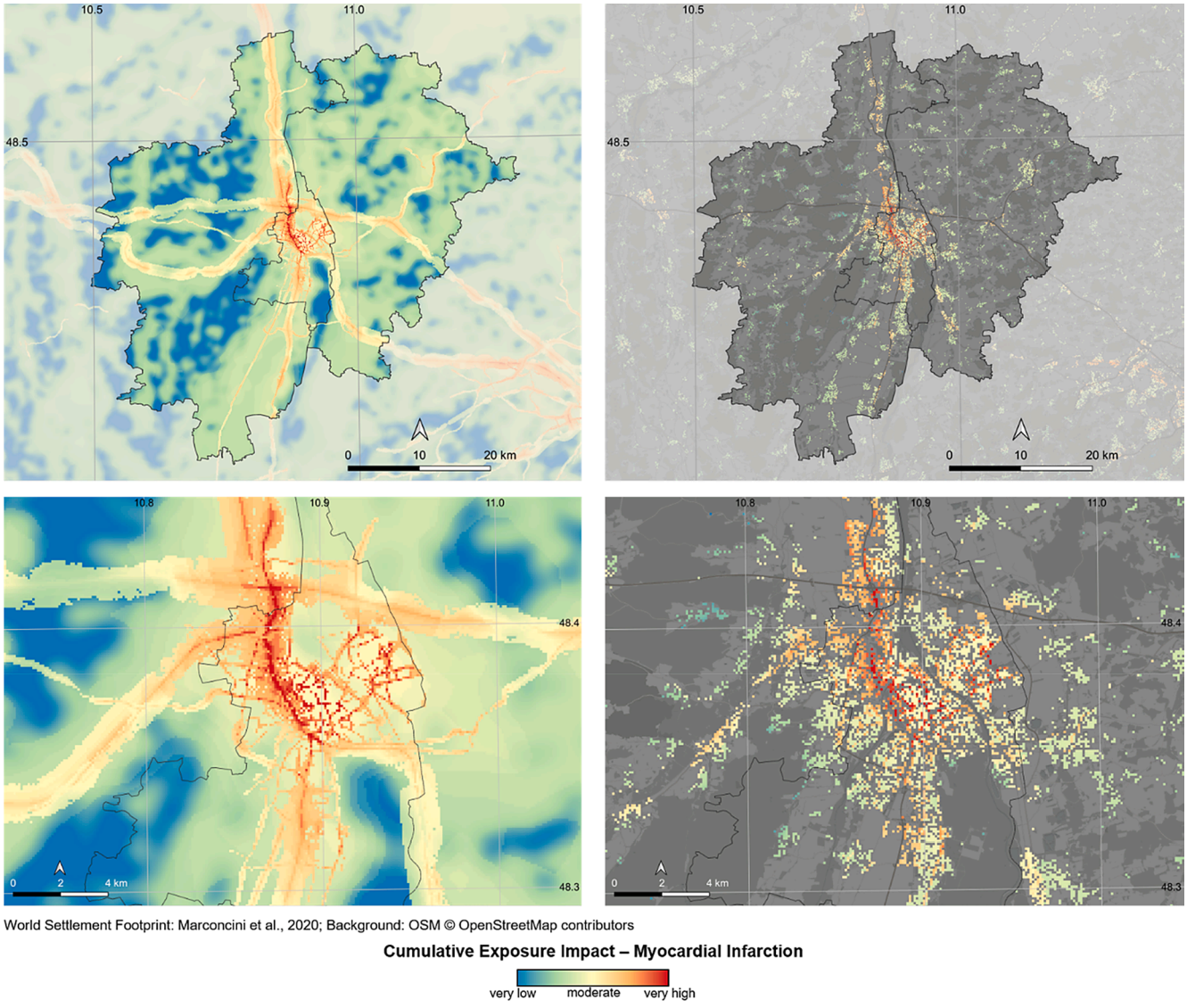

Fig. 6. Classified cumulative exposure impact for MI risk in the focus area. The upper two maps show the entire focus area, the lower two a zoomed-in view of Augsburg. The maps on the right show cumulative exposure impact only for built-up areas based on the World Settlement Footprint of 2015 (Marconcini et al., 2020).

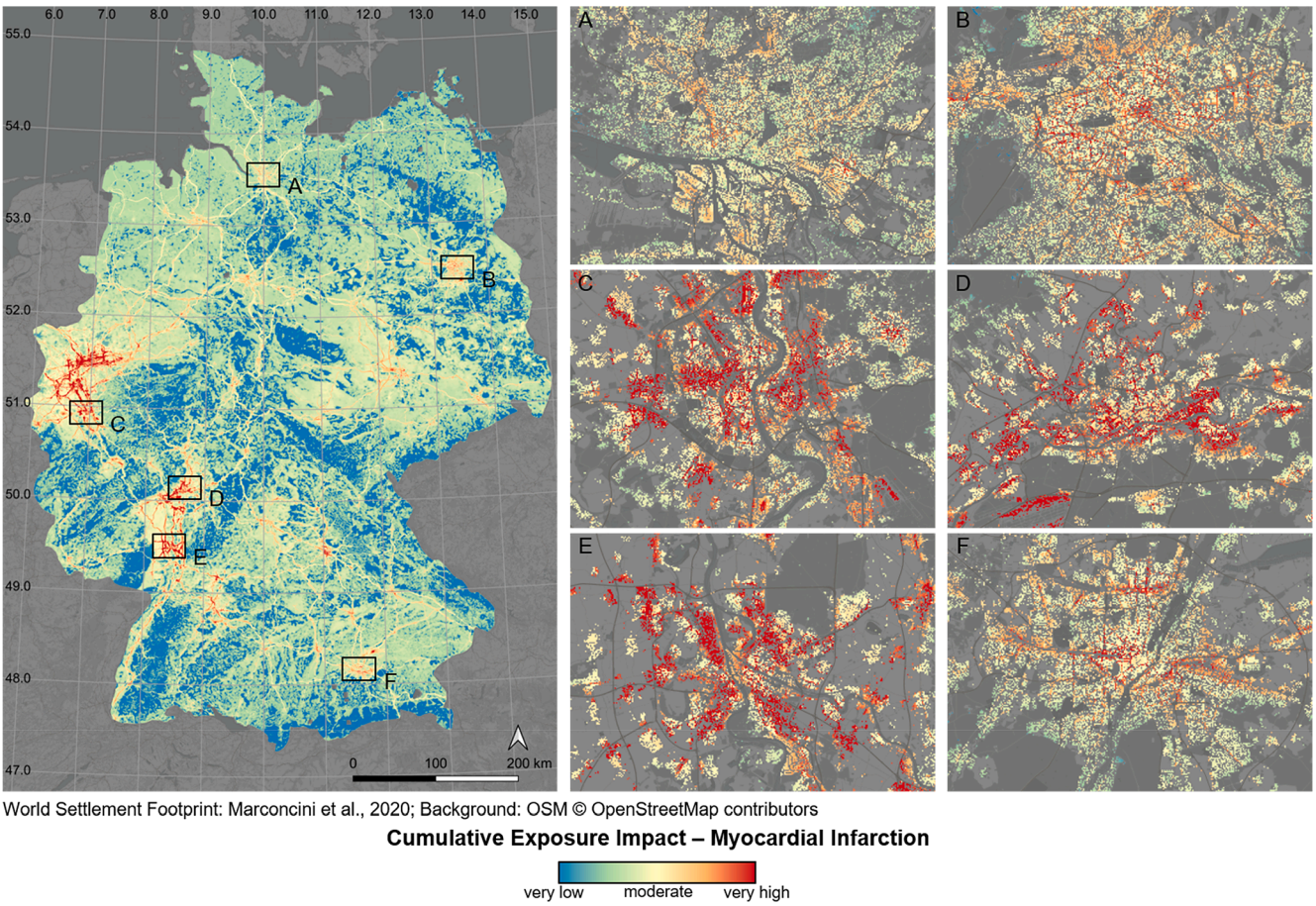

Fig. 7. Classified cumulative exposure impact for MI risk for all of Germany (left) and built-up areas of some major cities (right). Shown cities are Hamburg (A), Berlin (B), Cologne (C), Frankfurt am Main (D), Ludwigshafen & Mannheim (E), Munich (F).

burden for MI in Augsburg alone.

5.2. Spatial transferability

Previous approaches have been tested and adjusted to fit European cities (Mueller et al., 2017; Sicard et al., 2012). Our analysis and mapping approach uses and expands on previous approaches. We, therefore, propose it is transferable to other areas and timeframes and show the applicability of cumulative exposure impact maps for all of Germany, and major cities within the country (Fig. 7). The standardized scaling allows for easy comparability of exposure impact between cities.

Viewing the entire country, several exposure hotspots are visible. Especially the densely populated Ruhr valley (roughly 51° – 51.7° N, 6° – 7.5° E) and Upper Rhine valley (roughly 49° – 50.25° N, 8° – 9° E) stand out due to industrial activity. Apart from these major hotspots, larger cities are identifiable as clusters of high exposure. Further, busy highways and other noisy infrastructure are discernable as thin lines of elevated exposure impact. In contrast, there is little exposure in the forested uplands in the Southwest (e.g., the Black Forest at roughly 47.5° to 48.9° N, 7.5° to 8.8° E), along the Alps at the southern border, as well as in the center and east of Germany. These areas are sparsely populated and see little industrial activity. For the entire country, exposure impact is "very low" in ~ 19 %, "low" in ~ 66 %, "moderate" in ~ 13 %, "high" in ~ 2 %, and "very high" in < 1 % of the total mapped area. Only considering built-up areas, exposure impact is "very low" in ~ 1 %, "low" in ~ 54 %, "moderate" in ~ 32 %, "high" in ~ 10 %, and "very high" in ~ 3 %. Thus, populated areas generally have a higher cumulative exposure impact than non-populated areas.

Regarding the individual cities portrayed in Fig. 7, there is no apparent connection between city size and exposure impact. Berlin (B), Hamburg (A), and Munich (F) are the largest cities in the country with ~ 3.7 million, ~ 1.9 million, and ~ 1.6 million inhabitants, respectively. Except for built-up areas near busy streets and railways, exposure within these cities is mostly "moderate". Residents living in areas of "very high" exposure impact make up ≤ 0.5 % of the respective city population. Especially in Hamburg, a considerable portion of inhabitants lives in "low" exposure areas (36.1 %). In contrast, cities in traditionally industrial regions, like Cologne (C), Frankfurt (D), and the fused cities Ludwigshafen & Mannheim (E) are more exposed, despite having fewer inhabitants (~ 1.0 million in Cologne, ~ 0.8 million in Frankfurt, and a combined ~ 0.5 million in Ludwigshafen & Mannheim). In part, this is due to infrastructure with high exposure impact (such as large factory buildings for example). Additionally, regionally elevated exposure comes into play here. As indicated, especially along the Rhine and Ruhr valleys, there is much industrial activity and the area is largely urbanized. Accordingly, there is much noise pollution; concentrations of e.g., $PM_{2.5}$ and NO_2, as well as summer temperatures, are comparatively high. In urban areas, where exposure impact is generally higher than in surrounding rural settings, we, therefore, see large areas of "high" to "very high" exposure.

5.3. Comparison to external data

To explore the explanatory value of presented exposure results for total MI risk, we compare them to external data. For the study area, no data is available that communicates MI incidences. We utilize MI mortality on a county level instead, as this is the most up-to-date and high-resolution medical dataset available to us. This dataset is provided by

the Census Bureaus of the Federal States of Germany (Bayerisches Landesamt für Statistik, 2022; Statistische Ämter des Bundes und der Länder, 2018) and holds information on deaths and cause of death per county for 2019. We expect that this dataset is not a perfect fit for exposure impact values, as other factors besides environmental exposure impact MI mortality. To compare calculated exposure with MI mortality, we aggregate exposure impact in built-up areas per county to a mean value (Fig. 8). We then estimate the explanatory value from a Pearson correlation. Although the cumulative exposure impact shows only environmental exposure and does not consider external factors (e.g., availability of hospitals) or the impact of other NCD-relevant spheres (genome and behavior), it still has a non-dismissible explanatory value of $r = 0.23$ for MI deaths in Germany.

6. Discussion

Based on the findings of the last > 20 years of NCD research, we can say that the absence of vegetation and water in combination with high air-, noise-, and light pollution creates an unhealthy environment (Sogno et al., 2020). The entirety of these external factors – collectively addressed as exposome – is stressful for the human body and may trigger and worsen NCDs. We characterize the exposome and its spatial patterns as a sum of RR values of NCD-specific environmental factors. This evidence-based approach can help communicate the health burden such adverse environments have and the spatial patterns of NCD-relevant exposure.

6.1. Interpretation of exposure maps

In all presented exposure maps, the urban centers can be identified as the main exposure hotspots. Within those, especially industrially and commercially used areas exhibit elevated cumulative exposure impact values. Further, high-density built-up areas, busy streets, and railways stand out due to increased exposure impact. Near extensive urban green and blue spaces, exposure impact dips. Considering Augsburg as an example, many areas within the city have a “moderate” exposure impact. At and around parks and other recreational areas exposure is “low” to “very low”, while in areas close to busy downtown streets, industrial areas, or railway lines the exposure impact is “high” or “very high”. Exposure values in rural areas are generally lower than those within the city. Analogous to the situation within the city, exposure hotspots are largely associated with the presence of industrial land use or traffic noise. We conclude that for MI, the cumulative exposure impact is higher within the city than in its surroundings. Especially in cooler, forested areas, MI-relevant exposure can be minimized.

Urbanized areas are not to be considered bad for public health per se. As depicted in Fig. 7, cumulative exposure is relatively low for Hamburg, for example. Due to its extensive network of green and blue spaces, the impact of adverse environmental exposures is limited. On the other hand, it appears that cities with traditionally high industrial activity (like Cologne, Frankfurt am Main, Ludwigshafen & Mannheim) have a high cumulative exposure impact. For these three cities, we estimate that ~ 1.2 million people live in environments with “high” to “very high” MI-relevant exposure impact. Epidemiological evidence suggests that the affected local population has to bear a substantial health burden.

6.2. Validity of study findings

The produced exposure impact maps are based on a state-of-the-art approach (Sicard et al., 2012). Our calculations utilize epidemiological evidence from literature and transfer this knowledge to the spatial dimension. The presented results do not show or intend to show the risk of disease. For such a product, it would be necessary to include factors from the behavioral sphere as well (e.g., Mueller et al., 2017), since lifestyle choices like diet, drug consumption, or physical activity that are included in this sphere can have a more substantial impact on overall risk than the exposome. Tobacco smoking for example impacts the overall MI risk extremely: RR values reportedly range between 1.3 and 33, depending on sex, age, and the number of smoked cigarettes per day (e.g., Negri et al., 1994; Prescott et al., 1998). The impact of the behavioral and the genetic sphere thus limits the predictive value of exposure maps for NCD risk. Especially considering the strict regulations in place regarding e.g., the allowed concentration of air pollutants in Germany (Umweltbundesamt, 2022b), it may be expected that the effect of environmental exposure is drowned out by the impact of the other

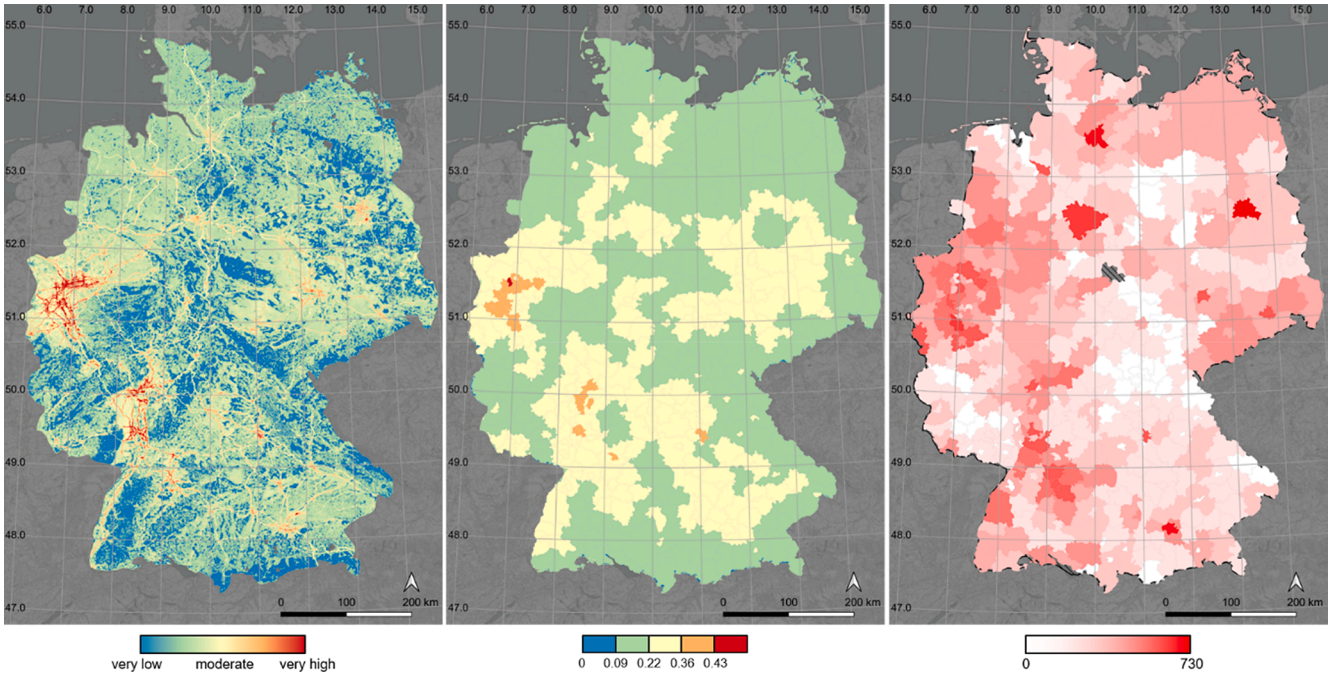

Fig. 8. Comparison of cumulative exposure impact for MI, aggregated cumulative exposure impact for built-up areas per county, and MI mortality per county (from left to right).

two spheres.

However, when compared to MI deaths in the study area, exposure values aggregated by county have a low but non-dismissible explanatory value of Pearson's r = 0.23. This value indicates that the produced exposure map can explain MI deaths to a certain degree, even without correcting for impacts from the behavioral or genetic sphere. This suggests that even in a country with strict environmental laws the little pollution that does exist impacts public health. At the same time, there is a lack of large-scale exposome maps. To our knowledge, we provide the first long-term exposure impact maps that are NCD-specific and include both land surface and air pollution parameters.

6.3. Optimization potential

There is a need for validated datasets that offer insight into near-ground air pollution for compounds besides $PM_{2.5}$ and NO_2. Air pollutants like near-surface O_3 and CO for example seem to impact public health (Sogno et al., 2020). So far, no products are available at an adequate spatial and temporal resolution that communicate near-surface concentrations of O_3 and CO for our study area. As soon as such products become available, they can be implemented into the presented workflow, further enhancing exposure estimates.

Employed datasets are in part static (e.g., noise pollution). Dynamic changes (e.g., the decrease in vehicle counts and consequentially traffic noise during the first months of COVID) are not quantifiable within those. More up-to-date data, which is currently not available, may therefore be beneficial for future studies.

Most RR values are extracted from large systematic reviews. Within those, not all considered studies focus on the same study area and there is variance in considered health outcomes. Accordingly, for the pooled RR values listed remains a degree of uncertainty that must be kept in mind when interpreting the cumulative exposure impact results.

Our approach follows the idea of a clear cause-response relationship between individual environmental factors and health outcomes, which has been previously applied in the field (e.g., Mueller et al., 2017; Sicard et al., 2011). Influences that exposure factors may have on each other are not considered.

A remaining challenge is data availability. Currently, no large-scale datasets are available for the investigated study region that communicate MI occurrence. We utilized census data on MI deaths to quantify the explanatory value of the produced exposure maps for MI risk, but this is not optimal as differences in external factors like medical infrastructure have an impact on MI mortality (Berlin et al., 2016). We hypothesize that comparison to MI incidences would yield a higher correlation coefficient.

6.4. Importance of study findings

Albeit their limitations, the presented results are important for understanding health-relevant environmental exposure and its spatial patterns. To our knowledge, there has not been any mapping effort equaling our approach in the number of environmental factors included or in the considered geographical scale. The novel exposure product presented is largely based on freely and globally available EO products. Our approach is therefore transferable to other regions and can provide health-relevant information in very high detail with individual streets and structures being identifiable. We emphasize that the presented maps merely show exposure impact, not NCD risk, which is also influenced by the genome and behavior. High cumulative exposure impact values may not directly translate to high NCD prevalence within the population, but they can help identify unhealthy (and healthy) environments. Within the context of this study, we have demonstrated our approach for MI. However, it can also be used for other diseases if given equations are adjusted according to the RR values listed in Table 1.

We propose such maps could be of use for public health services. Further, medical personnel, health agencies, and decision-makers have expressed interest in such a product as it allows them to base their considerations on an easy-to-interpret tool with profound thematic meaning (Brazeau and Ogden, 2022). Most importantly however, this product can be used to communicate a health burden that finds too little public awareness. Even more so since exposure to adverse environmental factors like PM cannot be accurately estimated based on intuition (Muñoz-Pizza et al., 2020).

7. Conclusion & outlook

Non-communicable diseases (NCDs) are a global problem. They are responsible for > 70 % of premature deaths, generate enormous economic losses, and reduce the quality of life for those affected. NCDs are known to be associated with environmental factors, collectively addressed as the exposome. Although a growing number of works in both the medical and Earth Observation (EO) field have been able to identify specific environmental impactors on human health, area-wide exposure products are not widely available so far. In this paper, we provide a transferable approach for long-term exposure impact mapping based on several health-impacting environmental factors. Namely, we investigate green space and blue space availability, light pollution, noise pollution, temperature, and air pollution ($PM_{2.5}$ and NO_2). We demonstrate our approach for exposures relevant to myocardial infarction risk. A transfer to other NCDs is possible using the relative risk values aggregated for this study. From our findings, we conclude that exposure impact is highest in highly urbanized areas and along major transport axes.

In our focus area of Augsburg, high exposure values are especially prominent in industrial areas, along main transport axes, and in areas with low surrounding greenness. In the city center, most areas only have "moderate" exposure, higher values are confined to busy streets and junctions. Accordingly, most of Augsburg's residents live in areas of "moderate" exposure (69 %). Still, the share of residents living in areas of "high" to "very high" exposure is considerable (18 %). In rural areas around the city, most people live in areas of "low" exposure. Transferring our approach to the rest of Germany, we can identify the cumulative exposure impact across the country. Especially in heavily industrialized areas, such as the Rhine and Ruhr valleys, exposure impact values are elevated. Urban populations in such areas bear a high health burden. For the cities Cologne, Frankfurt am Main, Ludwigshafen & Mannheim, a combined 1.2 million people live in areas of "high" to "very high" exposure impact. In total, exposure is "high" to "very high" for 13 % of the nation's built-up areas. These numbers demand increased efforts to reduce exposure to adverse environmental factors like air, noise, and light pollution.

It has to be emphasized that environmental exposure does not directly translate to NCD risk or NCD prevalence. For this, all NCD-relevant spheres (exposome, behavior, and genome) would have to be included. Although strict environmental regulations are in place for our study area that limit the concentration of harmful exposures, the cumulative exposure impact hints towards a low but non-dismissible impact on increased myocardial infarction deaths. This requires further investigation of the exposome's impact on human health. It is conceivable that the increased health burden has a noticeable effect on the local population, as well as health institutions and the economy.

We see application opportunities for exposome maps in the health and EO sectors, as well as beyond. We propose that especially in decision-making and sustainable urban planning they could be used to identify focus areas and monitor health-relevant environmental change.

Funding

HGF-HICAM Initiative.

CRediT authorship contribution statement

Patrick Sogno: Methodology, Visualization, Writing – original draft, Writing – review & editing. **Claudia Kuenzer:** Conceptualization, Supervision, Writing – review & editing. **Felix Bachofer:** Supervision, Writing – review & editing. **Claudia Traidl-Hoffmann:** Conceptualization, Supervision, Writing – review & editing.

Declaration of Competing Interest

The authors declare that they have no known competing financial interests or personal relationships that could have appeared to influence the work reported in this paper.

Data availability

Data will be made available on request.

Acknowledgments

This work was undertaken in the context of the Helmholtz-Climate Initiative Project (HI-CAM), funded by the Helmholtz Association, HGF.

References

Aschbacher, J., 2017. In: Satellite Earth Observations and Their Impact on Society and Policy. Springer Singapore, Singapore, pp. 81–86.
Bakour, C., Schwartz, S.W., Wang, W., Sappenfield, W.M., Couluris, M., Chen, H., O'Rourke, K., 2020. Sleep duration patterns from adolescence to young adulthood and the risk of asthma. Ann. Epidemiol. 49, 20–26. https://doi.org/10.1016/j.annepidem.2020.07.003.
Bayerisches Landesamt für Statistik, 2022. Bayerisches Landesamt für Statistik - GENESIS-Online [WWW Document]. URL https://www.statistikdaten.bayern.de/genesis/online (accessed 9.27.22).
Beck, H.E., Zimmermann, N.E., McVicar, T.R., Vergopolan, N., Berg, A., Wood, E.F., 2018. Present and future Köppen-Geiger climate classification maps at 1-km resolution. Sci. Data 5, 180214. https://doi.org/10.1038/sdata.2018.214.
Berlin, C., Panczak, R., Hasler, R., Zwahlen, M., 2016. Do acute myocardial infarction and stroke mortality vary by distance to hospitals in Switzerland? Results from the Swiss National Cohort Study. BMJ Open 6 (11), e013090. https://doi.org/10.1136/bmjopen-2016-013090.
Beverland, I.J., Cohen, G.R., Heal, M.R., Carder, M., Yap, C., Robertson, C., Hart, C.L., Agius, R.M., 2012. A comparison of short-term and long-term air pollution exposure associations with mortality in two cohorts in Scotland. Environ. Health Perspect. 120 (9), 1280–1285.
Borroni, E., Pesatori, A.C., Bollati, V., Buoli, M., Carugno, M., 2022. Air pollution exposure and depression: A comprehensive updated systematic review and meta-analysis. Environ. Pollut. 292, 118245 https://doi.org/10.1016/j.envpol.2021.118245.
Brazeau, S., Ogden, N.H. (Eds.), 2022. Earth observation, public health and one health: activities, challenges and opportunities. CABI, Wallingford.
Breiteneder, H., Diamant, Z., Eiwegger, T., Fokkens, W.J., Traidl-Hoffmann, C., Nadeau, K., O'Hehir, R.E., O'Mahony, L., Pfaar, O., Torres, M.J., Wang, D.Y., Zhang, L., Akdis, C.A., 2019. Future research trends in understanding the mechanisms underlying allergic diseases for improved patient care. Allergy 74, 2293–2311. https://doi.org/10.1111/all.13851.
Cai, Y., Ramakrishnan, R., Rahimi, K., 2021. Long-term exposure to traffic noise and mortality: A systematic review and meta-analysis of epidemiological evidence between 2000 and 2020. Environmental pollution (Barking, Essex : 1987) 269, 116222.
Chen, G., Wan, X., Yang, G., Zou, X., 2015. Traffic-related air pollution and lung cancer: A meta-analysis. Thoracic Cancer 6, 307–318. https://doi.org/10.1111/1759-7714.12185.
Chen, J., Hoek, G., 2020. Long-term exposure to PM and all-cause and cause-specific mortality: A systematic review and meta-analysis. Environ. Int. 143, 105974 https://doi.org/10.1016/j.envint.2020.105974.
Cheng, J., Xu, Z., Bambrick, H., Prescott, V., Wang, N., Zhang, Y., Su, H., Tong, S., Hu, W., 2019. Cardiorespiratory effects of heatwaves: A systematic review and meta-analysis of global epidemiological evidence. Environ. Res. 177, 108610 https://doi.org/10.1016/j.envres.2019.108610.
Cooper, M.J., Martin, R.V., Hammer, M.S., Levelt, P.F., Veefkind, P., Lamsal, L.N., Krotkov, N.A., Brook, J.R., McLinden, C.A., 2022. Global fine-scale changes in ambient NO2 during COVID-19 lockdowns. Nature 601, 380–387. https://doi.org/10.1038/s41586-021-04229-0.
Dendup, T., Feng, X., Clingan, S., Astell-Burt, T., 2018. Environmental Risk Factors for Developing Type 2 Diabetes Mellitus: A Systematic Review. Int. J. Environ. Res. Public Health 15 (1), 78.
Engemann, K., Pedersen, C.B., Arge, L., Tsirogiannis, C., Mortensen, P.B., Svenning, J.-C., 2019. Residential green space in childhood is associated with lower risk of psychiatric disorders from adolescence into adulthood. Proc. Natl. Acad. Sci. 116, 5188–5193. https://doi.org/10.1073/pnas.1807504116.
European Environmental Agency, 2022a. CLC 2018 [WWW Document]. URL https://land.copernicus.eu/pan-european/corine-land-cover/clc2018 (accessed 7.29.22).
European Environmental Agency, 2022b. Urban Atlas [WWW Document]. URL https://land.copernicus.eu/local/urban-atlas (accessed 7.27.22).
Gariazzo, C., Carlino, G., Silibello, C., Tinarelli, G., Renzi, M., Finardi, S., Pepe, N., Barbero, D., Radice, P., Marinaccio, A., Forastiere, F., Michelozzi, P., Viegi, G., Stafoggia, M., Carla, A., Paola, A., Stefania, A., Sandra, B., Lucia, B., Michela, B., Sergio, B., Laura, B., Serena, B., Giuseppe, B., Simone, B., Giuseppe, C., Giuseppe, C., Achille, C., Antonio, C., Annamaria, C., de' Donato Francesca, Salvatore, F., Sandro, F., Francesco, F., Claudia, G., Claudio, G., Paolo, G.R., Stefania, L.G., Gaetano, L., Sara, M., Alessandro, M., Paola, M., Enrica, M., Antonino, M., Alessandro, N., Marta, O., Federica, P., Nicola, P., Paola, R., Andrea, R., Matteo, R., Salvatore, S., Matteo, S., Camillo, S., Roberto, S., Massimo, S., Gianni, T., Francesco, U., Giovanni, V., 2021. Impact of different exposure models and spatial resolution on the long-term effects of air pollution. Environ. Res. 192, 110351 https://doi.org/10.1016/j.envres.2020.110351.
Gehring, U., Tamburic, L., Sbihi, H., Davies, H.W., Brauer, M., 2014. Impact of noise and air pollution on pregnancy outcomes. Epidemiology (Cambridge 25 (3), 351–358.
Gorelick, N., Hancher, M., Dixon, M., Ilyushchenko, S., Thau, D., Moore, R., 2017. Google Earth Engine: Planetary-scale geospatial analysis for everyone. Remote Sens. Environ. 202, 18–27. https://doi.org/10.1016/j.rse.2017.06.031.
Grandner, M.A., Patel, N.P., Gehrman, P.R., Perlis, M.L., Pack, A.I., 2010. Problems associated with short sleep: Bridging the gap between laboratory and epidemiological studies. Sleep Med. Rev. 14, 239–247. https://doi.org/10.1016/j.smrv.2009.08.001.
Guzinski, R., Nieto, H., 2019. Evaluating the feasibility of using Sentinel-2 and Sentinel-3 satellites for high-resolution evapotranspiration estimations. Remote Sens. Environ. 221, 157–172. https://doi.org/10.1016/j.rse.2018.11.019.
Ha, S., Hu, H., Roussos-Ross, D., Haidong, K., Roth, J., Xu, X., 2014. The effects of air pollution on adverse birth outcomes. Environ. Res. 134, 198–204.
He, D., Wu, S., Zhao, H., Qiu, H., Fu, Y., Li, X., He, Y., 2017. Association between particulate matter 2.5 and diabetes mellitus: A meta-analysis of cohort studies. J. Diabet. Investig. 8, 687–696. https://doi.org/10.1111/jdi.12631.
Holliday, E.G., Magee, C.A., Kritharides, L., Banks, E., Attia, J., 2013. Short sleep duration is associated with risk of future diabetes but not cardiovascular disease: a prospective study and meta-analysis. PLoS ONE 8, e82305.
Huang, C., Nichols, C., Liu, Y., Zhang, Y., Liu, X., Gao, S., Li, Z., Ren, A., 2015. Ambient air pollution and adverse birth outcomes: a natural experiment study. Popul. Health Metrics 13, 17.
Huangfu, P., Atkinson, R., 2020. Long-term exposure to NO2 and O3 and all-cause and respiratory mortality: A systematic review and meta-analysis. Environ. Int. 144, 105998 https://doi.org/10.1016/j.envint.2020.105998.
Jacobeit, J., 1990. Neuere Daten und Faktren zum Stadtklima von Augsburg. In: Fischer, K. (Ed.), Beiträge Zur Physichen Geographie Des Raumes Augsburg. Klaus Fischer, pp. 1–27.
Kim, K.Y., Lee, E., Kim, Y.J., Kim, J., 2017. The association between artificial light at night and prostate cancer in Gwangju City and South Jeolla Province of South Korea. Chronobiol. Int. 34, 203–211.
Kim, Y.S., Park, D.K., Hwang, I.C., Ahn, H.Y., 2018. Daily Weather Conditions and Anticipated Death from Cancer. Iran. J. Public Health 47, 591–596.
Kottek, M., Grieser, J., Beck, C., Rudolf, B., Rubel, F., 2006. World Map of the Köppen-Geiger climate classification updated. Meteorol. Z. 15, 259–263. https://doi.org/10.1127/0941-2948/2006/0130.
Lee, H.Y., Wu, C.D., Chang, Y.T., Chern, Y.R., Lung, S.C., Su, H.J., Pan, W.C., 2020. Association between Surrounding Greenness and Mortality: An Ecological Study in Taiwan. Int. J. Environ. Res. Public Health 17. https://doi.org/10.3390/ijerph17124525.
Lin, Y.-K., Ho, T.-J., Wang, Y.-C., 2011. Mortality risk associated with temperature and prolonged temperature extremes in elderly populations in Taiwan. Environ. Res. 111, 1156–1163.
Liu, Q., Wang, W., Gu, X., Deng, F., Wang, X., Lin, H., Guo, X., Wu, S., 2021. Association between particulate matter air pollution and risk of depression and suicide: a systematic review and meta-analysis. Environ. Sci. Pollut. Res. 28, 9029–9049. https://doi.org/10.1007/s11356-021-12357-3.
Liu, Y., Yan, S., Zou, L., Wen, J., Fu, W., 2022. Noise exposure and risk of myocardial infarction incidence and mortality: a dose-response meta-analysis. Environ. Sci. Pollut. Res. Int. 29, 46458–46470.
Manjarrés, A.D., 2009. Edge-Preserving Image Upscaling (Master of Science). University of California, Irvine.
Marconcini, M., Metz-Marconcini, A., Üreyen, S., Palacios-Lopez, D., Hanke, W., Bachofer, F., Zeidler, J., Esch, T., Gorelick, N., Kakarla, A., Paganini, M., Strano, E., 2020. Outlining where humans live, the World Settlement Footprint 2015. Sci. Data 7, 242. https://doi.org/10.1038/s41597-020-00580-5.
Mueller, N., Rojas-Rueda, D., Basagaña, X., Cirach, M., Cole-Hunter, T., Dadvand, P., Donaire-Gonzalez, D., Foraster, M., Gascon, M., Martinez, D., Tonne, C., Triguero-Mas, M., Valentín, A., Nieuwenhuijsen, M., 2017. Urban and Transport Planning Related Exposures and Mortality: A Health Impact Assessment for Cities. Environ. Health Perspect. 125, 89–96. https://doi.org/10.1289/ehp220.
Muñoz-Pizza, D.M., Villada-Canela, M., Reyna, M.A., Texcalac-Sangrador, J.L., Serrano-Lomelin, J., Osornio-Vargas, Á., 2020. Assessing the Influence of Socioeconomic Status and Air Pollution Levels on the Public Perception of Local Air Quality in a

Mexico-US Border City. Int. J. Environ. Res. Public Health 17. https://doi.org/10.3390/ijerph17134616.
Mustafić, H., Jabre, P., Caussin, C., Murad, M.H., Escolano, S., Tafflet, M., Périer, M.-C., Marijon, E., Vernerey, D., Empana, J.-P., Jouven, X., 2012. Main Air Pollutants and Myocardial Infarction: A Systematic Review and Meta-analysis. JAMA 307, 713–721. https://doi.org/10.1001/jama.2012.126.
Negri, E., La Vecchia, C., Nobili, A., D'Avanzo, B., Bechi, S., 1994. Cigarette smoking and acute myocardial infarction. Eur J Epidemiol 10, 361–366. https://doi.org/10.1007/BF01719657.
Neumeier, S., 2013. Modellierung der Erreichbarkeit öffentlicher Apotheken: Untersuchung zum regionalen Versorgungsgrad mit Dienstleistungen der Grundversorgung (Thünen Working Papers No. 14). Johann Heinrich von Thünen Institute, Federal Research Institute for Rural Areas, Forestry and Fisheries.
Paksarian, D., Rudolph, K.E., Stapp, E.K., Dunster, G.P., He, J., Mennitt, D., Hattar, S., Casey, J.A., James, P., Merikangas, K.R., 2020. Association of Outdoor Artificial Light at Night With Mental Disorders and Sleep Patterns Among US Adolescents. JAMA Psychiatry 77, 1266–1275.
Patel, P.C., 2019. Light pollution and insufficient sleep: Evidence from the United States. Am. J. Human Biol. 31, e23300.
Prescott, E., Hippe, M., Schnohr, P., Hein, H.O., Vestbo, J., 1998. Smoking and risk of myocardial infarction in women and men: longitudinal population study. BMJ 316, 1043. https://doi.org/10.1136/bmj.316.7137.1043.
Pun, V.C., Kazemiparkouhi, F., Manjourides, J., Suh, H.H., 2017. Long-Term PM2.5 Exposure and Respiratory, Cancer, and Cardiovascular Mortality in Older US Adults. Am. J. Epidemiol. 186, 961–969. https://doi.org/10.1093/aje/kwx166.
Ring, J., Akdis, C., Lauener, R., Schäppi, G., Traidl-Hoffmann, C., Akdis, M., Ammann, W., Behrendt, H., Bieber, T., Biedermann, T., Bienenstock, J., Blaser, K., Braun-Fahrländer, C., Brockow, K., Buters, J., Crameri, R., Darsow, U., Denburg, J. A., Eyerich, K., Frei, R., Galli, S.J., Gutermuth, J., Holt, P., Koren, H., Leung, D., Müller, U., Muraro, A., Ollert, M., O'Mahony, L., Pawankar, R., Platts-Mills, T., Rhyner, C., Rosenwasser, L.J., Schmid-Grendelmeier, P., Schmidt-Weber, C.B., Schmutz, W., Simon, D., Simon, H.U., Sofiev, M., van Hage, M., van Ree, R., 2014. Global Allergy Forum and Second Davos Declaration 2013 Allergy: Barriers to cure – challenges and actions to be taken. Allergy 69, 978–982. https://doi.org/10.1111/all.12406.
Rojas-Rueda, D., Nieuwenhuijsen, M.J., Gascon, M., Perez-Leon, D., Mudu, P., 2019. Green spaces and mortality: a systematic review and meta-analysis of cohort studies. The Lancet. Planetary health 3, e469–e477.
Roswall, N., Raaschou-Nielsen, O., Ketzel, M., Overvad, K., Halkjær, J., Sørensen, M., 2017. Modeled traffic noise at the residence and colorectal cancer incidence: a cohort study. Cancer Causes Control : CCC 28, 745–753.
Sabrin, S., Karimi, M., Nazari, R., 2020. Developing Vulnerability Index to Quantify Urban Heat Islands Effects Coupled with Air Pollution: A Case Study of Camden. NJ. ISPRS Int. J. Geo-Inform. 9 https://doi.org/10.3390/ijgi9060349.
Scherber, K., Langner, M., Endlicher, W.R., 2014. Spatial analysis of hospital admissions for respiratory diseases during summer months in Berlin taking bioclimatic and socio-economic aspects into account. DIE ERDE – J. Geogr. Soc. Berlin 144, 217–237.
Schifano, P., Cappai, G., De Sario, M., Michelozzi, P., Marino, C., Bargagli, A.M., Perucci, C.A., 2009. Susceptibility to heat wave-related mortality: a follow-up study of a cohort of elderly in Rome. Environ. Health 8, 50. https://doi.org/10.1186/1476-069X-8-50.
Schwarz, N., Schlink, U., Franck, U., Großmann, K., 2012. Relationship of land surface and air temperatures and its implications for quantifying urban heat island indicators—An application for the city of Leipzig (Germany). Ecol. Ind. 18, 693–704. https://doi.org/10.1016/j.ecolind.2012.01.001.
Shin, H.H., Maquiling, A., Thomson, E.M., Park, I.-W., Stieb, D.M., Dehghani, P., 2022. Sex-difference in air pollution-related acute circulatory and respiratory mortality and hospitalization. Sci. Total Environ. 806, 150515 https://doi.org/10.1016/j.scitotenv.2021.150515.
Shin, J., Choi, J., Kim, K.J., 2019. Association between long-term exposure of ambient air pollutants and cardiometabolic diseases: A 2012 Korean Community Health Survey. Nutrition, Metabol. Cardiovasc. Dis. 29, 144–151. https://doi.org/10.1016/j.numecd.2018.09.008.
Sicard, P., Lesne, O., Alexandre, N., Mangin, A., Collomp, R., 2011. Air quality trends and potential health effects – Development of an aggregate risk index. Atmos. Environ. 45, 1145–1153. https://doi.org/10.1016/j.atmosenv.2010.12.052.
Sicard, P., Talbot, C., Lesne, O., Mangin, A., Alexandre, N., Collomp, R., 2012. The Aggregate Risk Index: An intuitive tool providing the health risks of air pollution to health care community and public. Atmos. Environ. 46, 11–16. https://doi.org/10.1016/j.atmosenv.2011.10.048.
da Silveira, I.H., Junger, W.L., 2018. Green spaces and mortality due to cardiovascular diseases in the city of Rio de Janeiro. Rev. Saude Publica 52, 49.
Sogno, P., Traidl-Hoffmann, C., Kuenzer, C., 2020. Earth Observation Data Supporting Non-Communicable Disease Research: A Review. Rem. Sens. 12, 2541. https://doi.org/10.3390/rs12162541.
Son, J.-Y., Lee, J.-T., Lane, K.J., Bell, M.L., 2019. Impacts of high temperature on adverse birth outcomes in Seoul, Korea: Disparities by individual- and community-level characteristics. Environ. Res. 168, 460–466.
Song, X., Jiang, L., Zhang, D., Wang, X., Ma, Y., Hu, Y., Tang, J., Li, X., Huang, W., Meng, Y., Shi, A., Feng, Y., Zhang, Y., 2021. Impact of short-term exposure to extreme temperatures on diabetes mellitus morbidity and mortality? A systematic review and meta-analysis. Environ. Sci. Pollut. Res. 28, 58035–58049. https://doi.org/10.1007/s11356-021-14568-0.
Statistische Ämter des Bundes und der Länder, 2018. Gestorbene nach Geschlecht und ausgewählten Todesursachen -Jahr - regionale Ebenen (bis 2019) [WWW Document]. GovData. URL https://www.govdata.de/daten/-/details/gestorbene-nach-geschlecht-und-ausgewahlten-todesursachen-jahr-regionale-ebenen (accessed 9.27.22).
Sun, S., Weinberger, K.R., Nori-Sarma, A., Spangler, K.R., Sun, Y., Dominici, F., Wellenius, G.A., 2021. Ambient heat and risks of emergency department visits among adults in the United States: time stratified case crossover study. BMJ (Clinical research ed.) 375, e065653.
Sun, Z., Chen, C., Xu, D., Li, T., 2018. Effects of ambient temperature on myocardial infarction: A systematic review and meta-analysis. Environ. Pollut. 241, 1106–1114. https://doi.org/10.1016/j.envpol.2018.06.045.
Teoh, K.K., Ibrahim, H., Bejo, S.K., 2008. Investigation on several basic interpolation methods for the use in remote sensing application. 2008 IEEE Conference on Innovative Technologies in Intelligent Systems and Industrial Applications 60–65.
Tobías, A., Díaz, J., Saez, M., Carlos Alberdi, J., 2001. Use of Poisson regression and Box-Jenkins models to evaluate the short-term effects of environmental noise levels on daily emergency admissions in Madrid, Spain. Eur. J. Epidemiol. 17, 765–771. https://doi.org/10.1023/A:1015663013620.
Tomlinson, C.J., Chapman, L., Thornes, J.E., Baker, C.J., 2011. Including the urban heat island in spatial heat health risk assessment strategies: a case study for Birmingham, UK. Int. J. Health Geogr. 10, 42. https://doi.org/10.1186/1476-072X-10-42.
Turner, M.C., Nieuwenhuijsen, M., Anderson, K., Balshaw, D., Cui, Y., Dunton, G., Hoppin, J.A., Koutrakis, P., Jerrett, M., 2017. Assessing the Exposome with External Measures: Commentary on the State of the Science and Research Recommendations. Annu. Rev. Public Health 38, 215–239. https://doi.org/10.1146/annurev-publhealth-082516-012802.
Twohig-Bennett, C., Jones, A., 2018. The health benefits of the great outdoors: A systematic review and meta-analysis of greenspace exposure and health outcomes. Environ. Res. 166, 628–637. https://doi.org/10.1016/j.envres.2018.06.030.
Umweltbundesamt, 2022a. Lärmkartierung nach der EU-Umgebungslärmrichtlinie [WWW Document]. URL https://gis.uba.de/maps/resources/apps/laermkartierung/index.html?lang=de (accessed 6.14.22).
Umweltbundesamt, 2022b. Hintergrund Februar 2022: Luftqualität 2021. Umweltbundesamt, Dessau-Roßlau.
van Donkelaar, A., Hammer, M.S., Bindle, L., Brauer, M., Brook, J.R., Garay, M.J., Hsu, N.C., Kalashnikova, O.V., Kahn, R.A., Lee, C., Levy, R.C., Lyapustin, A., Sayer, A.M., Martin, R.V., 2021. Monthly Global Estimates of Fine Particulate Matter and Their Uncertainty. Environ. Sci. Technol. 55, 15287–15300. https://doi.org/10.1021/acs.est.1c05309.
Van Kempen, E., Casas, M., Pershagen, G., Foraster, M., 2018. WHO Environmental Noise Guidelines for the European Region: A Systematic Review on Environmental Noise and Cardiovascular and Metabolic Effects: A Summary. Int. J. Environ. Res. Public Health 15. https://doi.org/10.3390/ijerph15020379.
Villeneuve, P.J., Lam, S., Tjepkema, M., Pinault, L., Crouse, D.L., Osornio-Vargas, A.R., Hystad, P., Jerrett, M., Lavigne, E., Stieb, D.M., 2022. Residential proximity to greenness and adverse birth outcomes in urban areas: Findings from a national Canadian population-based study. Environ. Res. 204, 112344.
WHO Regional Office for Europe, 2009. Night noise guidelines for Europe. World Health Organization Europe, Denmark.
Windsperger, K., Kiss, H., Oberaigner, W., Leitner, H., Binder, F., Muin, D.A., Foessleitner, P., Husslein, P.W., Farr, A., 2022. Exposure to night-time light pollution and risk of prolonged duration of labor: A nationwide cohort study. Birth 49, 87–96. https://doi.org/10.1111/birt.12577.
World Health Organization, 2021. Noncommunicable diseases [WWW Document]. Noncommunicable diseases. URL https://www.who.int/news-room/fact-sheets/detail/noncommunicable-diseases (accessed 7.29.22).
Zhu, Z., Wulder, M.A., Roy, D.P., Woodcock, C.E., Hansen, M.C., Radeloff, V.C., Healey, S.P., Schaaf, C., Hostert, P., Strobl, P., Pekel, J.-F., Lymburner, L., Pahlevan, N., Scambos, T.A., 2019. Benefits of the free and open Landsat data policy. Remote Sens. Environ. 224, 382–385. https://doi.org/10.1016/j.rse.2019.02.016.